Computer Methods and Programs in Biomedicine 270 (2025) 108913

Contents lists available at ScienceDirect

Computer Methods and Programs in Biomedicine

journal homepage: https://www.sciencedirect.com/journal/computer-methods-and-programs-in-biomedicine

HybridDLDR: A hybrid deep learning-based drug resistance prediction system of Glioblastoma (GBM) using molecular descriptors and gene expression data

Sajid Naveed [a,*], Mujtaba Husnain [b], Najah Alsubaie [c]

[a] Department of Computer Science, Faculty of Computing, The Islamia University of Bahawalpur, 63100, Pakistan
[b] Department of Information Technology, Faculty of Computing, The Islamia University of Bahawalpur, 63100, Pakistan
[c] Department of Computer Sciences, College of Computer and Information Sciences, Princess Nourah bint Abdulrahman University (PNU), Riyadh, 11671, Saudi Arabia

ARTICLE INFO

Dataset link: https://github.com/xajidnaveedofficial/HybridDLDR.git, https://www.cancerrxgene.org/

Keywords:
Glioblastoma (GBM)
Hybrid deep learning
Drug resistance prediction
Molecular descriptors
Gene expression

ABSTRACT

Background and Objective: Glioblastoma (GBM), a very aggressive type of brain tumor, sometimes creates a chemoresistant state that compromises the effectiveness of chemotherapy and leads to serious clinical complications in treatment. Predicting drug resistance is crucial for the improvement of medication effect during cancer treatment. Assessing drug resistance is difficult due to the pricey chemotherapeutic trails and prolonged laboratory investigations. Deep learning plays a significant role in drug resistance prediction nowadays.

Methods: This paper presents a novel deep learning model that combines Convolutional Neural Networks (CNN), Long Short Term Memory Networks (LSTM), and transformer architectures to predict drug resistance. The proposed application acts as a system that estimate the resistance of drugs based on gene expression details and chemical properties.

Results: As compared with existing model for drug resistance prediction, proposed model achieved lower Mean Squared Error (MSE) of 0.4109 and Mean Absolute Error (MAE) of 0.5040, along with higher R^2 of 0.9635 and pearson correlation of 0.9999.

Conclusions: This work significantly advances the fields of pharmacogenomics and personalized medicine through an in-depth evaluation that includes complex performance metrics and visualizations.

1. Introduction

According to Gottesman et al. (2023) GBM is very aggressive type of brain tumor, Sometimes it creates a chemoresistant state that negatively affects the results of chemotherapy. The interaction of epigenetic and genetic features has been investigated as an important factor in drug resistance in GBM, demonstrating the complexity of this type of cancer [1]. Some GBM-related genes develop chemoresistance during treatment [2].

In order to address the issue of drug resistance, personalized treatments are necessitated and require an understanding of drug resistance pathways [3]. Although resistance to personalized medication in GBM remains an obstacle that requires further exploration of the underlying molecular pathways, these drugs have shown promise in treating the disease [4]. The optimal treatment for GBM could be selected by evaluating the drug resistance in cancer genes. Advanced cancer treatments with Half Maximal Inhibitory Concentrations (IC50) have also been practiced nowadays [5]. Expression promoter methylation and circadian regulation of MGMT may be a factor that increases chemosensitivity in GBM treatment [6]. Sensitivity to chemotherapy is promoted by GBM stem cells, which have the unique ability to self-renew and show lower resistance to chemotherapy [7].

Since Trim25 inhibited further cleavage of ITPKB, the glioma was also resistant to chemotherapy [2]. Personalized medicine has marked the emergence of a new approach to medicine where treatment, management strategies, and diagnostic methods are the cure for an individual's cancer type and stage [2]. By using biological markers, oncologists can ensure that their approaches are more targeted by personalized medicine based on the unique genetic changes found in malignancies [8]. Precision oncology is a promising application of personalized medicine that personalizes cancer treatment by applying genetic and molecular data. [9]. A model that precisely responds to certain characteristics in a personalized way (a method known as personalized

* Corresponding author.
E-mail address: xajidnaveed@gmail.com (S. Naveed).

https://doi.org/10.1016/j.cmpb.2025.108913
Received 24 September 2024; Received in revised form 11 May 2025; Accepted 13 June 2025
Available online 27 June 2025
0169-2607/© 2025 The Authors. Published by Elsevier B.V. This is an open access article under the CC BY-NC-ND license (http://creativecommons.org/licenses/by-nc-nd/4.0/).

medicine) is an admirable strategy for managing malignancy [10]. Personalized medicine has introduced an innovative way to treat cancer based on the genetics and circumstances of patients [11].

The main difference between personalized medicine and traditional treatments is that personalized treatments are designed specifically based on genetic mutations and the degree of drug sensitivity [12]. Sometimes, due to drug resistance similar medicines and treatments do not work for similar symptoms and conditions. Personalized medicine then plays an significant role in predicting the amount of drug resistance to a particular chemotherapy [13]. Because this type of therapy is based on genetic mutation, it is also effective in reducing the side effects and reactions with other drugs. The method, which represents a paradigm shift in healthcare towards personalized care, involves evaluating massive volumes of data about medical history, lifestyle, genetic, and environmental factors to decide the best course of action for cancer patients [14].

Precision medicine has great potential, but as complex diseases involve many genetic and non-genetic risk factors and heterogeneous patients, there are obstacles along the way. Drug resistance is a major obstacle in the development of anticancer drugs and in the treatment of cancer [15]. Estimation of drug resistance plays an leading role in optimizing the effect of drug treatment [16]. Deep learning models utilizing gene expression are not only useful for cancer treatments but are also widely used in drug design, drug resistance, and biomarker identification [17]. The majority of GBM patients show resistance to almost all traditional therapies [18]. Predicting drug resistance is crucial to the improvement of personalized medicine [19].

AI-based drug sensitivity prediction models face several obstacles, including overfitting, interpretation issues, integration challenges with heterogeneous data, and the need for improved predictive accuracy [16]. In addition, some prediction models are complicated to understand and apply in clinical settings [20], making it difficult to understand the prediction process. Moreover, the complexity of diseases such as cancer, which involve complex genetic networks, is challenging because previous researches has focused on individual genes rather than their interactions [21]. When it comes to drug sensitivity (efficacy) prediction using multiple omics data, the task of coming up with complex criteria that can be used to develop and evaluate the most suitable machine learning models is not an easy task. This is another aspect that makes it even more complicated [22]. We need to address these questions to develop reliable predictive models relevant to personalized medicine and innovations in precision oncology. By predicting the resistance of cancer genes, the combination of computer algorithms can accelerate the search for drugs to treat GBM [23]. Deep learning holds a significant role in drug resistance prediction using multi-omic data to improve model interpretation and accuracy [24–26]. These models accurately predict resistance to cancer therapies using various data sources, including gene expressions, copy number variations, gene mutations, and metabolic expressions [27]. Researchers can extract highly interpretable biological information through the use of deep learning approaches such as deep neural networks and decision tree-based algorithms. This allows scientists to accurately predict the resistance of nonspecific and targeted anticancer drugs. Also, by incorporating drug-target interaction data through fused neural networks, the performance of existing deep learning-based drug resistance prediction models is further improved, especially for situations involving unknown drugs, showing remarkable improvements in correlation coefficient performance.

This research paper presents a new hybrid deep learning model that makes use of three deep learning architectures in order to predict drug resistance. We bring together CNN, LSTM, and transformer architectures as additive ingredients that enable analysis and interpretation of gene expression profiles besides molecular fingerprints.

2. Related work

Drug resistance prediction is one of the important areas in drug discovery, as it assistances for finding the most suitable treatments according to individual's gene expression. Thus, existing techniques and models are being established to address the concern of estimating the drug resistance. The Boundary Privileged Knowledge Distillation (BPKD) technique is the one that has been proposed [25]. This method solves the issue of poor learner edge predictions in dense prediction tasks through spatial boundary impedance information. BPKD concentrates on border sites to enhance the precision in the prediction of drug resistance patterns [28].

Experts have identified a straightforward but productive method to improve the overall efficacy of drug resistance prediction approaches and enhance their accuracy. By using graph-based non-autoregressive reaction prediction models like ReactionSink have effectively predicted suitable drug compositions during medical treatment [29]. The integration of ReactionSink doubly stochastic self-attention maps enables high-accuracy simultaneous sampling, which is valuable in calculating drug resistance. In the field of molecular property prediction (MPP), approaches using graph structure learning (GSL) have been developed to exploit relationships between genes and molecules for more accurate predictions [29]. In addition, Graph Multi-Similarity Learning (GraphMSL), a molecular property prediction framework, was developed and proven effective in drug development screening [30]. In 2023, Calmet et al. worked with a variety of different spray input parameters to improve drug delivery to the nose through targeting spray deposition using resistance analysis and machine learning [31]. This study exhibited that predictive models can improve the treatment efficiency of traditional medical practices by optimizing drug-targeting strategies. Shi et al. (2023) made a vast bioinformatics exploration to reveal the oncogenic role of FoxM1 in osteosarcoma [32]. Their findings highlight the importance of genetic and molecular markers in predicting treatment outcomes and have important implications for drug resistance, regulation of the immune microenvironment, and prognosis.

In the same way, Zhang et al. (2023) built an in-depth gene signature model focused on HGLRGs to predict drug resistance, immune resistance, metabolic characteristics, and survival in gastric cancer. This approach intends to fuse multidimensional data to improve forecast accuracy [33]. Wang et al. (2024) demonstrated the potential of fusing genetic and metabolomic data to improve drug resistance predictions by cross-referencing gene expression patterns with sphingolipid metabolism genes to predict prognosis and therapeutic resistance in patients with GBM [34]. In lung cancer, Chen et al. (2024) discovered genomic clusters with an acetylation-related ncRNA fingerprint that can more accurately estimate the cancer stage by using epigenome mutations on cancer drug [35]. Lu et al. (2024) predict alteration of psychological state of a cancer patient due to side effect of a cancer drugs using gene expression [36]. Pan et al. (2024) utilize biomarkers of immune system for estimate the effects of medication [37]. The research conducted by Wang et al. utilize spectrometer for forecast the medication effects for hypertension [38]. Naveed et al. [39] utilized K-mer fragmentation of drug SMILES with the Light Gradient Boosting Machine (LightGBM) to build a system for recommending the most effective drug.

In addition, Zhou et al. (2024) observed variations in gene expression of GBM patients due to chemo-drug [40]. The researchers used ML based model for prognostic the effect of medical treatment [18]. Predicting drug resistance for various diseases is one of the trending topic of scientific researches nowadays. They include using perceptual similarity that reduces proprietary data with bounds, graph-based non-autoregressive resistance prediction, and graph structure learning. AI-based systems and models are smart enough to diagnose drug resistance.

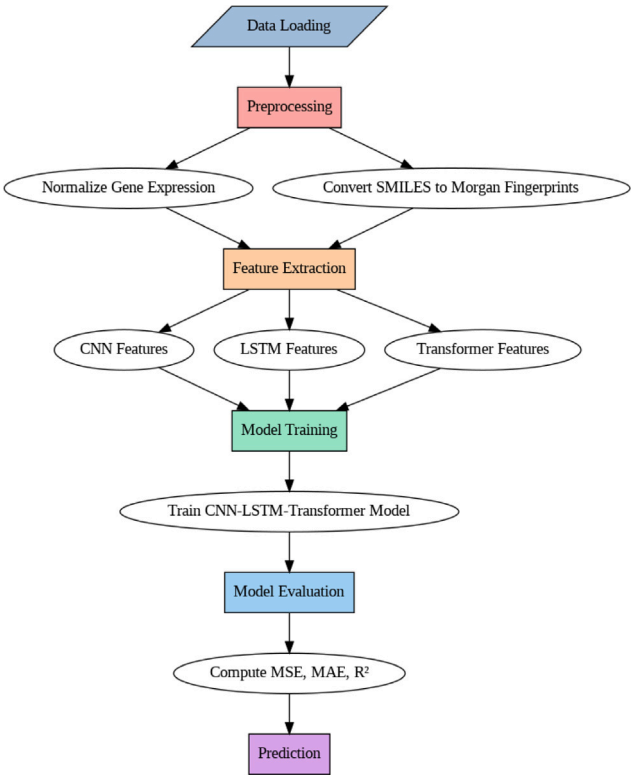


Fig. 1. Workflow of proposed methodology.

A crucial aspect of personalized medicinal care is the prediction of drug resistance, a critical factor in determining how efficient therapies are in treating different types of cancer. Personalized medicine gets the best possible therapy outcomes because it tailors treatments for patients based on their unique genetic and molecular characteristics. Although improving the accuracy and reliability of prediction models is still in progress, most studies highlight its importance in cancer treatment.

3. Materials and methods

The use of molecular descriptors and gene expression data will help develop an AI and deep learning-based recommendation system used to predict resistance to drug reactions, after which a series of steps will be followed, as outlined below (see Fig. 1).

3.1. Data source

The primary dataset for our research is The Genomics of Drug Sensitivity in Cancer (GDSC) [41]. The main goal of the GDSC project is a comprehensive database linking the molecular properties of cancer genes to their resistances to a wide range of therapeutic drugs. GDSC facilitates the identification of drug resistance biomarkers and the design of precision medicine strategies by integrating gene expression, inhibitory concentration (IC50) values, and molecular descriptors. Furthermore, we utilize the data from the Cancer Genome Atlas Program (TCGA) [42]. This dataset contains classified information on all 30 cancer types. We only selected data on GBM cancer.

3.2. Data preprocessing

Incorporating gene molecular descriptors with expression data deals a noteworthy advantage by providing a more general consideration of drug resistance methods. Gene expression data discloses the cell response to drug experience, emphasizing alterations in gene activity

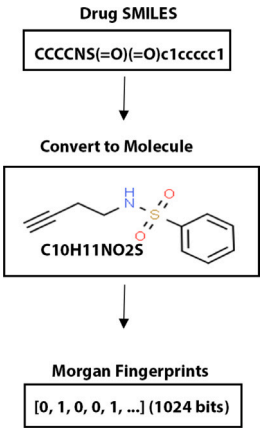


Fig. 2. Process of drugs SMILES to morgan fingerprints.

that cause drug resistance. On the other hand, molecular descriptors detention the physicochemical properties of drug combinations, which effect their interactions with target molecules and cellular components. By combining these data types, we capture both the biological context of resistance (gene expression) and the chemical context of drug action (molecular descriptors), allowing the model to identify difficult, multi-faceted resistance mechanisms that are often neglected when relying on either data type alone. This incorporated approach allows for a more precise and broad prediction of drug resistance, leading to improved insights for drug development and precision medication strategies.

3.2.1. Molecular descriptors

Molecular descriptors or drug SMILES strings are transformed to 1024-bit morgan vector fingerprints using RDKit. This technique produces a binary vector indicating the presence or absence of molecular substructures

3.2.2. Morgan fingerprint

Morgan fingerprints, also called circular fingerprints, are commonly used for demonstrating the chemical compositions of a drug (see Fig. 2).

These fingerprints utilize the connections of atoms in a chemical compound.

Steps for Morgan Fingerprint Construction

$$\text{Identifier}_i = f(\text{atom}_i) \tag{1}$$

$$\text{Identifier}_i^{(r)} = g\left(\text{Identifier}_i^{(r-1)},\ \left\{\text{Identifier}_j^{(r-1)} : j \in \mathcal{N}(i)\right\}\right) \tag{2}$$

$$\text{bitvector}\left[h\left(\text{Identifier}_i^{(r)}\right)\right] = 1 \tag{3}$$

$$\text{Morgan Fingerprint} = \begin{cases} V \\ \text{for all } i \in \text{Identifiers} \end{cases} \quad \text{bitvector}_i \tag{4}$$

Where:

- atom_i : The ith atom in the molecule.
- Identifier_i : Initial identifier assigned to atom i.
- $f(\cdot)$: Function that computes the initial identifier from atomic features.
- $\text{Identifier}_i^{(r)}$: Identifier of atom i at iteration (or radius) r.
- $g(\cdot)$: Update function that aggregates the identifier of atom i with those of its neighboring atoms.
- $\mathcal{N}(i)$: Set of neighboring atoms of atom i.
- $\text{bitvector}[h(\cdot)]$: Binary vector where the index determined by the hash function is set to 1.

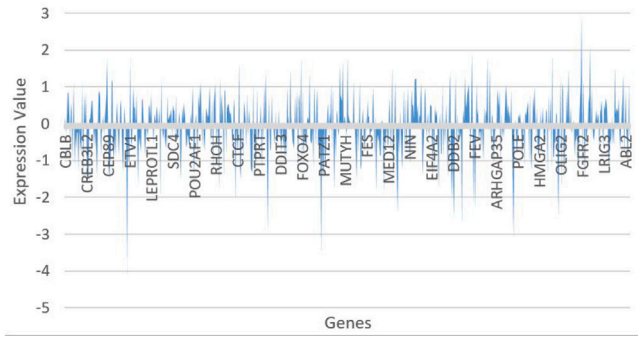


Fig. 3. Gene Expression representation of sample ID 687586 from the GDSC dataset.

- $h(\cdot)$: Hashing function that maps a compound identifier to a unique bit position.
- bitvector_i : Bit vector representation for atom i after hashing.
- Morgan Fingerprint : Final fingerprint vector V representing the molecule, obtained by aggregating all hashed identifiers.

3.2.3. Gene expression data

Gene expression data: StandardScaler is used to standardize all gene expression (see Fig. 3) features to mean 0 and 1 standard deviation. Model convergence and performance are improved with this scaling.

3.2.4. Data fusion

Data fusion involves merging synthetic gene expression data with molecular descriptors to create a single input matrix.

3.3. Model construction

The hybrid model combines three distinct deep learning architectures to capture different features of the input data: CNN for molecular descriptors, LSTM for gene expression data, and Transform for complex interactions (see Fig. 4).

3.3.1. CNN (molecular descriptors)

CNN are utilized to analyze chemical descriptors (see Fig. 4). First, 1024-bit morgan fingerprints are provided to the network, indicating that a molecule can have more than one substructure. These fingerprints represent the structure of each molecule as a binary vector of fixed size. The multiple convolutional layers of the CNN architecture are applied to extract hierarchical features from the input fingerprints. We introduce a maximum level of aggregation between these layers to reduce the spatial dimensions of the data, thereby minimize the risk of overfitting and reducing the computational complexity. The product of the process of clusters and convolutions is a feature map that is transformed into a one-dimensional vector. The final output layer passes this flattened vector through several dense (fully connected) layers. This model increases the predictive capabilities of CNN, particularly for tasks such as drug resistance testing, enabling it to recognize complex patterns or associations present among chemical descriptors.

Steps for CNN Construction for Molecular Descriptors

$$\text{Input Shape} = (1024) \tag{5}$$

$$(x * W + b)[i,j] = \sum_{m=0}^{M-1} (x[i, j+m] \cdot W[m]) + b \tag{6}$$

$$f(z) = \begin{cases} z, & \text{if } z \geq 0 \\ 0.01z, & \text{if } z < 0 \end{cases} \tag{7}$$

$$x_1 = \text{MaxPooling1D}(\text{size} = 3)(x_1) \tag{8}$$

$$p[i,j] = \max\left(x_1[i,j], x_1[i,j+1], x_1[i,j+2]\right) \tag{9}$$

$$x_1 = \text{Flatten}(x_1) \tag{10}$$

$$\text{Flatten}(X) = X_{\text{vector}} \tag{11}$$

$$x = \text{Dense}(32,\ \text{activation} = \text{LeakyReLU})(x_1) \tag{12}$$

$$z = W \cdot x_1^{\text{vector}} + b \tag{13}$$

$$f(z) = \begin{cases} z, & \text{if } z \geq 0 \\ 0.01z, & \text{if } z < 0 \end{cases} \tag{14}$$

$$x_1 = \text{Dropout}(0.025)(x_1) \tag{15}$$

$$x_1[i] = \begin{cases} x_1[i], & \text{with probability } 1 - 0.025 \\ 0, & \text{with probability } 0.025 \end{cases} \tag{16}$$

Where:

- x : Scalar input value.
- X : Vector or matrix input.
- x_1 : Intermediate feature representation.
- W : Weight matrix used in convolution or dense layer.
- b : Bias vector added after linear transformation.
- i, j : Indices representing spatial positions in input or feature maps.
- m : Filter index used in convolutional operations.
- Convolution : Operation to extract local features using filters.
- MaxPooling1D : Reduces spatial dimensions by selecting maximum values in 1D segments.
- $\max(\cdot)$: Function that returns the maximum of a set of inputs.
- Flatten : Transforms multidimensional input into a 1D vector.
- Dense(32) : Fully connected neural network layer with 32 output units.
- z : Output before applying the activation function.
- $f(z)$: Activation function, here using LeakyReLU.
- Dropout(0.025) : Regularization technique that randomly sets 2.5

3.3.2. LSTM (gene expression data)

LSTM networks process gene expression values depending on standardized gene expression profiles. These profiles are processed to ensure that the expression level of each gene is consistent between samples (see Fig. 5).

The first two LSTM layers capture long-range interactions and temporal dependencies within the ordered gene expression samples. This arrangement makes it possible for AI models to recognize genetic indicators for GBM tumors; it also allows it to quickly predict drug reactions through detecting regularities and associations among genetic facts. The ability of LSTM layers to maintain memories over long ranges makes them capable of encompassing intricate interconnectedness in gene expressions. For that reason, this desired outcome becomes true in that following LSTM layer outputs, dense or fully connected layers receive it as features at once .

Steps for LSTM Construction for Gene Expression Data

$$\text{Input Shape} = \left(\mathbf{X}_{\text{Train}}.\text{Shape}[1] - 1024,\ 1\right) \tag{17}$$

$$x_2 = \text{LSTM}(16,\ \text{return_sequences} = \text{True})(\text{gene_input}) \tag{18}$$

$$f_t = \sigma(W_f \cdot [h_{t-1}, x_t] + b_f) \tag{19}$$

$$i_t = \sigma(W_i \cdot [h_{t-1}, x_t] + b_i) \tag{20}$$

$$\tilde{C}_t = \tanh(W_c \cdot [h_{t-1}, x_t] + b_c) \tag{21}$$

$$\sigma_t = \sigma(W_o \cdot [h_{t-1}, x_t] + b_o) \tag{22}$$

$$C_t = f_t \odot C_{t-1} + i_t \odot \tilde{C}_t \tag{23}$$

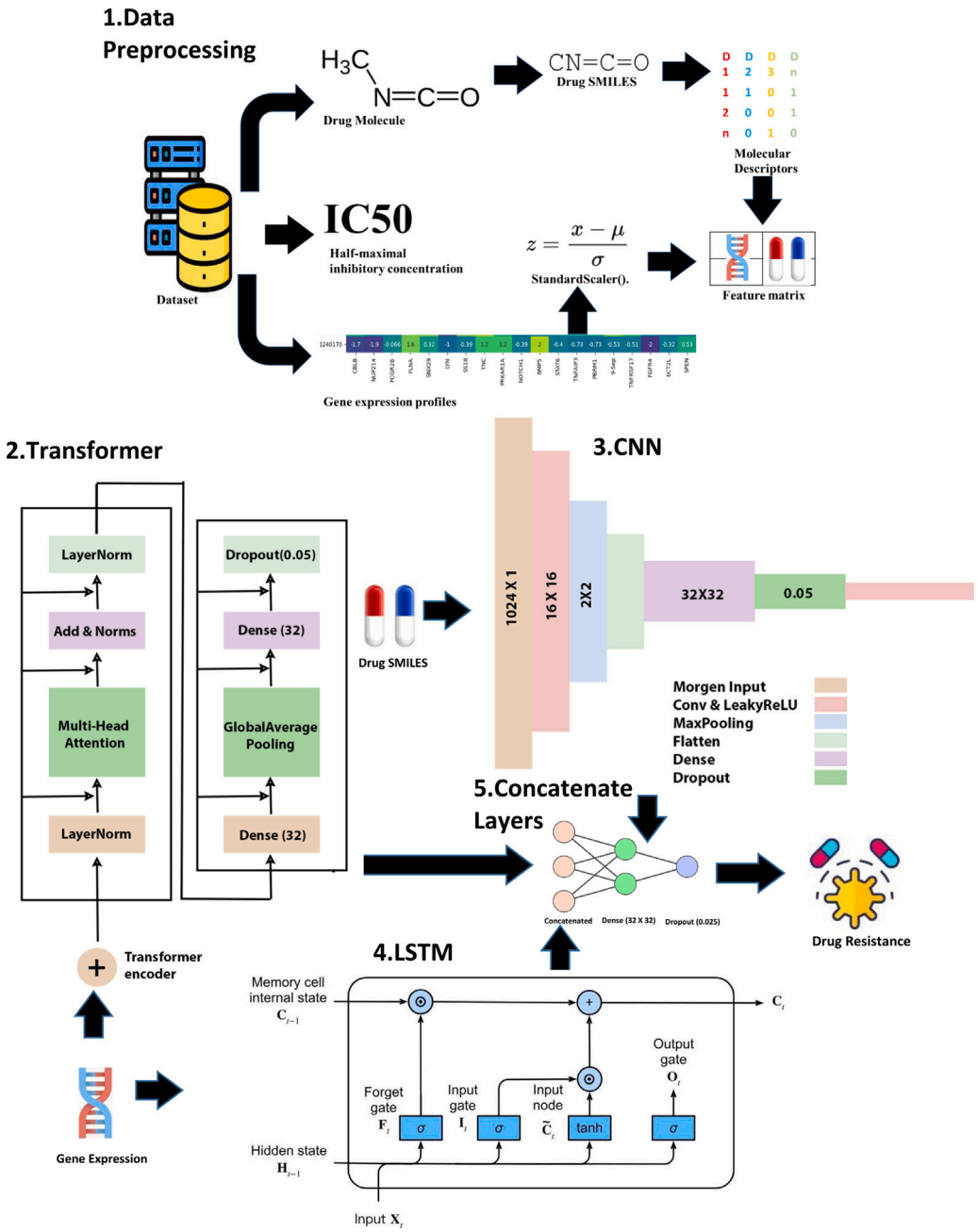


Fig. 4. Overview of the Hybrid Deep Learning-Based Drug Resistance Prediction System. The framework integrates molecular descriptors and gene expression data through three parallel deep learning branches. (1) In the preprocessing step, SMILES are converted into molecular descriptors, gene expression data are standardized, and all features are merged into a unified matrix for model input. (2) A Transformer encoder for capturing complex dependencies in gene expression, (3) a CNN for SMILES-derived molecular fingerprints, (4) an LSTM for sequential gene expression features. (5) The outputs are concatenated and processed through fully connected layers to predict drug resistance.

$$h_t = \sigma_t \odot \tanh(C_t) \tag{24}$$

$$x_2 = \text{LSTM}(16)(x_2) \tag{25}$$

$$x_2 = \text{Dense}(32,\ \text{activation} = \text{LeakyReLU})(x_2) \tag{26}$$

$$x_2 = \text{Dropout}(0.025)(x_2) \tag{27}$$

Where:

- $\mathbf{X}_{\text{Train}}$.Shape[1] : Number of training sequences.
- x_t : Input at current time step t.
- h_{t-1} : Hidden state from previous time step.
- f_t : Output of the forget gate.
- i_t : Output of the input gate.
- $\tilde{C}_t$: Candidate memory cell.
- C_t : Final cell state at time t.
- h_t : Hidden state at time t (also LSTM output).
- σ : Sigmoid activation function.
- tanh : Hyperbolic tangent activation function.
- W_f, W_i, W_c, W_o : Weight matrices for forget, input, candidate, and output gates respectively.
- b_f, b_i, b_c, b_o : Bias terms for each respective gate.
- $\odot$: Element-wise (Hadamard) product.
- LSTM(16) : LSTM layer with 16 hidden units.
- Dense(32) : Fully connected layer with 32 neurons.
- Dropout(0.025) : Regularization layer that randomly drops 2.5
- x_2 : Intermediate feature representation.

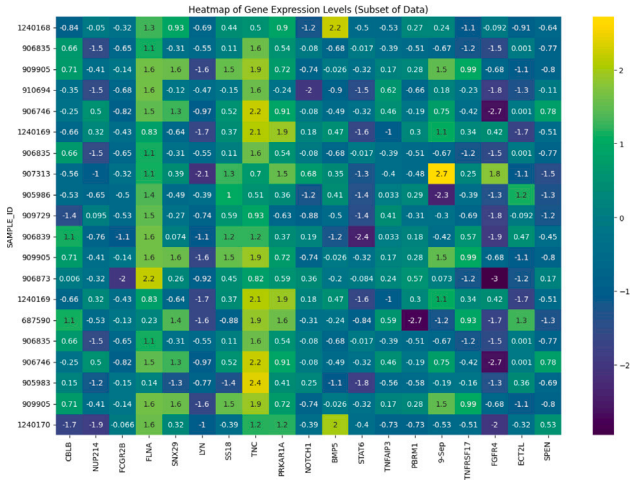


Fig. 5. Gene expression values of different samples from GDSC dataset.

3.3.3. Transformer (gene expression data)

We standardized the gene expression profiles for transformer model input using the GDSC dataset. We preprocessed these profiles to standardize gene expression levels across samples. The transformer architecture processes this data through several encoder layers. A multi-head attention mechanism incorporated in each encoder layer allows the model to simultaneously focus on different areas of the gene expression profile, thus capturing complex genetic connections and interactions. Layers of feedback neural networks are applied to refine and modify the representations produced. Feedback layers improve the model's ability to recognize non-linear patterns, and multi-head focus allows the model to dynamically determine the relative importance of different genes and their interactions. The transformer's complex construction makes it a valuable tool for examining drug reactions, diseases and identifying critical genes. The program can be used to conduct a thorough analysis of genetic and expression data.

Steps for Transformer Construction for Gene Expression Data

$$\text{Input Shape} = \left(\mathbf{X}_{\text{Train}}.\text{Shape}[1] - 1024,\ 1\right) \tag{28}$$

$$x_3 = \text{Transformer_Encoder}(x) \tag{29}$$

$$\text{LN}(x) = \frac{x - \mu}{\sqrt{\sigma^2 + \epsilon}} \tag{30}$$

$$\text{Attention}(Q, K, V) = \text{softmax}\left(\frac{QK^\top}{\sqrt{d_k}}\right)V \tag{31}$$

$$\text{FFN}(x) = \max\left(0,\ xW_1 + b_1\right)W_2 + b_2 \tag{32}$$

$$x_3 = \text{GlobalAveragePooling1D}(x_3) \tag{33}$$

$$x_3 = \text{Dense}(32,\ \text{activation} = \text{LeakyReLU})(x_3) \tag{34}$$

$$x_3 = \text{Dropout}(0.025)(x_3) \tag{35}$$

Where:

- $\mathbf{X}_{\text{Train}}.\text{Shape}[1]$: Number of training sequences.
- x : Input feature at a given position (scalar or vectorized).
- x_3 : Output of the Transformer encoder block after processing.
- μ : Mean of input vector x.
- σ^2 : Variance of input vector x.
- ϵ : Small constant to prevent division by zero during normalization.
- $Q = XW_Q$: Query matrix (projection of input).
- $K = XW_K$: Key matrix (projection of input).
- $V = XW_V$: Value matrix (projection of input).
- d_k : Dimension of the key vectors.
- $\text{Attention}(Q, K, V)$: Scaled dot-product attention result.
- $\text{LN}(x)$: Layer normalization output.
- $\text{FFN}(x)$: Position-wise feed-forward network applied after attention.
- W_1, W_2 : Weight matrices of the dense layers in FFN.
- b_1, b_2 : Bias vectors of the dense layers in FFN.
- GlobalAveragePooling1D : Reduces dimensionality by averaging across all positions.
- Dense(32) : Fully connected layer with 32 output neurons.
- Dropout(0.025) : Regularization technique that randomly zeroes out 2.5

3.3.4. Concatenate layers

These layers combine outputs from transformers, LSTMs, and CNNs to create a unified model representation. CNN models can relate mRNA quantities to temporal correlations by extracting information from descriptors, while transform models interpret complex relationships. Combining the capabilities of CNN, LSTM and transformer in a multifaceted way. Following it through some connected layers further processes and fuses the data. After that, these deep layers use dropout regularization, which randomly removes some neurons during training to increase model generalization and reduce overfitting .

Steps for Concatenate Construction

$$\text{Concatenated} = \text{Concatenate}(\left[x_1, x_2, x_3\right]) \tag{36}$$

$$x = \text{Dense}(32, \text{activation} = \text{LeakyReLU})(\text{Concatenated}) \tag{37}$$

$$x = \text{Dropout}(0.025)(x) \tag{38}$$

$$\text{Output} = \text{Dense}(1)(x) \tag{39}$$

Where:

- Concatenate : Combines the outputs of multiple models into a single tensor.
- $[x_1, x_2, x_3]$: Outputs from CNN, LSTM, and Transformer models.
- Dense(32) : Fully connected layer with 32 neurons.
- x : Value after dropout regularization.
- LeakyReLU : Activation function applied to the output of the dense layer.

3.4. Model training

3.4.1. Training setup

The MSE loss function, which quantifies the RMSE difference between predicted and real values, is a convenient tool for regression tasks such as estimating IC50 values and is used in model training. Model weights are optimized by Adam optimizer, with a learning rate of 0.05, to strike a balance between stability and efficient convergence. Two important enhancement mechanisms are append to improve training efficiency and avoid overfitting: Plateau learning rate reduction (which reduces the learning rate when validation loss stagnates and allows finer adjustments) and early termination (which stops training when the performance on the validation set stops improving).

3.4.2. Training procedure

80% of the split was used in training, and 20% was retained for the testing phase, the model performance evaluation in the while-training–validation set. The proposed model rationalizes the weights during training and manages the inputs through callbacks, which constantly assess its progress on the validation data. This hybrid model aims to construct a noteworthy prediction model for estimate the resistance in IC50 values by utilizing the concatenating molecular and genomic data.

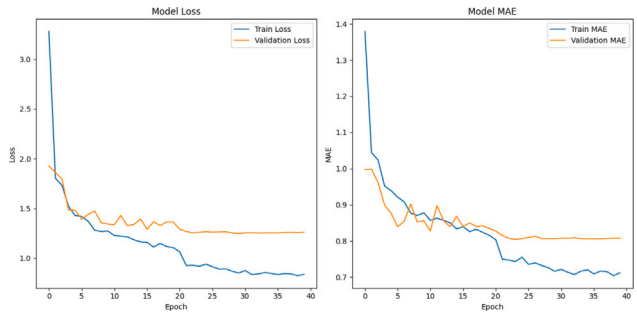


Fig. 6. Model training and validation loss.

3.4.3. Model evaluation and validation

The proposed model improved the training loss by 0.8372, and MAE by 0.7122. The model reduced the valid loss by 1.2608 and valid MAE loss by 0.8076 (see Fig. 6).

3.4.4. Robustness of the methodology

To improve the generalizability s and robustness our model, we incorporated multiple regularization techniques, including learning rate reduction, dropout, and early stopping. Dropout was integrated at many layers of the CNN, LSTM, and Transformer components to avoid overfitting by randomly deactivating neurons during training, thereby imposing the model to learn more generalizable features. We applied a dropout rate of 0.05 across different layers to balance effective learning and regularization. Early stopping was employed to monitor validation loss, confirming that the model training halts once performance begins to degrade on unseen data. This avoids overfitting while maintaining computational effectiveness. Moreover, learning rate reduction on plateau was utilized to adaptively drop the learning rate if no enhancement in validation loss was detected. This gradual reduction allows the model to converge more efficiently by fine-tuning the weight updates in later training phases. Together, these methods contribute to the model's robustness, confirming that it not only learns complex patterns effectively but also generalizes well to unseen data. This organized approach reduces the risk of overfitting and improves the model's reliability for real-world applications.

3.4.5. Computational resources and training parameters

For this study, we trained our model using an NVIDIA A100 GPU with 40 GB VRAM, running on a high-performance computing (HPC) cluster with 256 GB RAM and 64-core AMD EPYC processors. The training process took approximately 14 h for 100 epochs with a batch size of 2, leveraging TensorFlow and Keras as the primary deep learning frameworks. Despite optimizations, real-world deployment in clinical settings or drug discovery pipelines may require further model compression techniques, such as quantization or pruning, to improve inference speed and reduce computational overhead. Moreover, hyperparameters such as the number of LSTM units (16), Transformer heads (4), feed-forward dimension (32), and CNN filters (16) were optimized through grid search experiments.

4. Results

The proposed research intended to estimate chemo-drug resistance on GBM samples with gene expression, drug molecular descriptors via SMILES using CNN, LSTM, and transformer deep learning models. We combines three state-of-the-art neural network architectures in a suitable composition for increase efficacy of the system. We used transformer models for identifying complex genetic interactions, LSTM networks for capturing temporal dependencies in gene expression data, and CNN for processing molecular descriptors. This fusion strategy exploits the advantages of each model in order to come up with a thorough analysis framework for prediction. The outcomes demonstrate the clinically acceptable accuracy across different chemo-drugs. HybridDLDR performance was evaluated by coefficient of determination (R^2), MAE, MSE and Pearson Correlation. The proposed model performed well with MSE 0.4109, MAE 0.5040, and R^2 value 0.9635 and Pearson Correlation value 0.9999 (see Fig. 24). The outcomes show that this model performed with acceptable accuracy. Fig. 7 shows overall difference between real and predicted IC50 values. Fig. 8 shows Linear Regression analysis graph of real and predicted IC50 values. Fig. 9 shows distribution of residual in real and prediction.

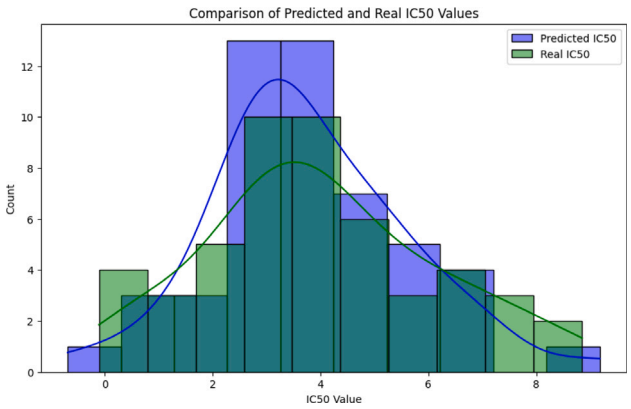


Fig. 7. Overall difference between real and predicted IC50 values.

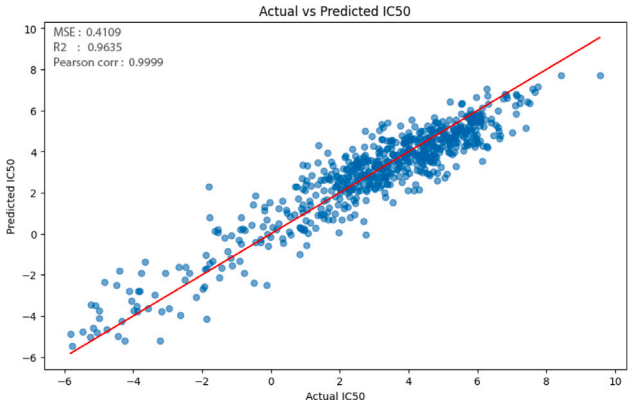


Fig. 8. Linear regression analysis between real and predicted IC50 values of the proposed system, showing MSE, R^2, and Pearson correlation.

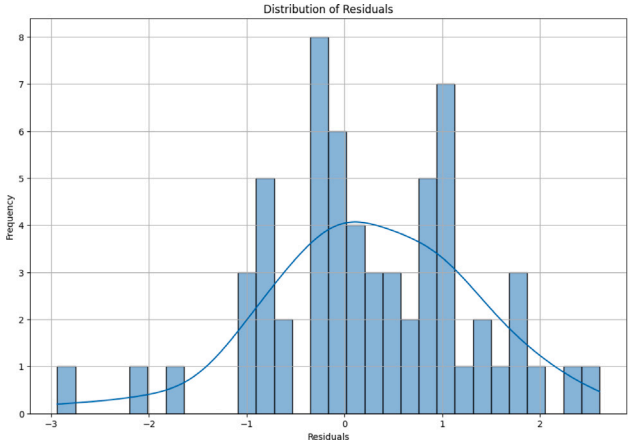


Fig. 9. Distribution of residual values of IC50.

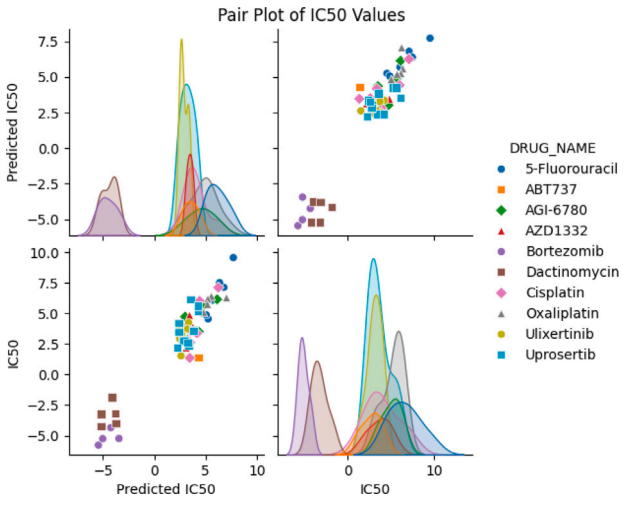


Fig. 10. Pair plot of different cancer drugs.

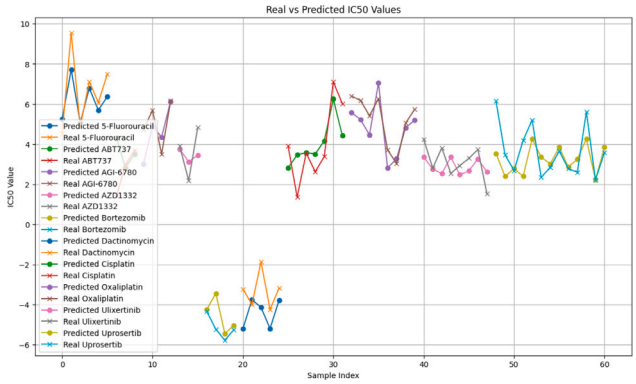


Fig. 11. Real and predicted IC50 values of cancer drugs.

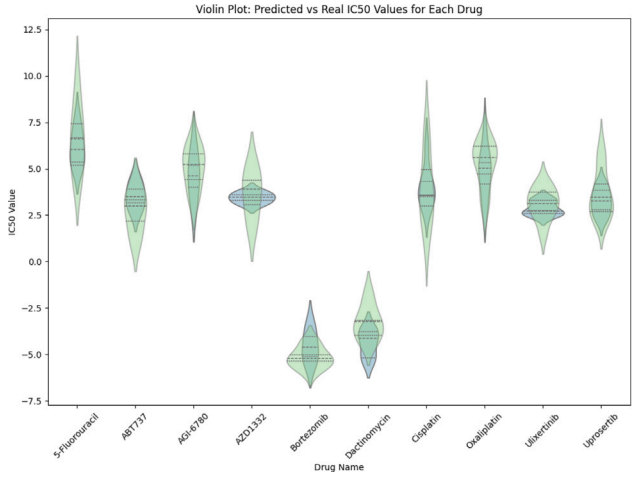


Fig. 12. Difference between real and predicted IC50 values of cancer drugs.

Fig. 10 shows pair plot of different drugs for deep analysis of the efficacy of the system. Figs. 11, 12 & 13 demonstrate the real and predicted values of IC50 for different chemo-drugs. Fig. 14 shows the real values of IC50 with their related drugs and Fig. 15 shows predicted values of IC50 with their related drugs.

For the chemo-drug namely 5-Fluorouracil, the proposed hybrid model was precisely forecasting the resistance, with a minor difference

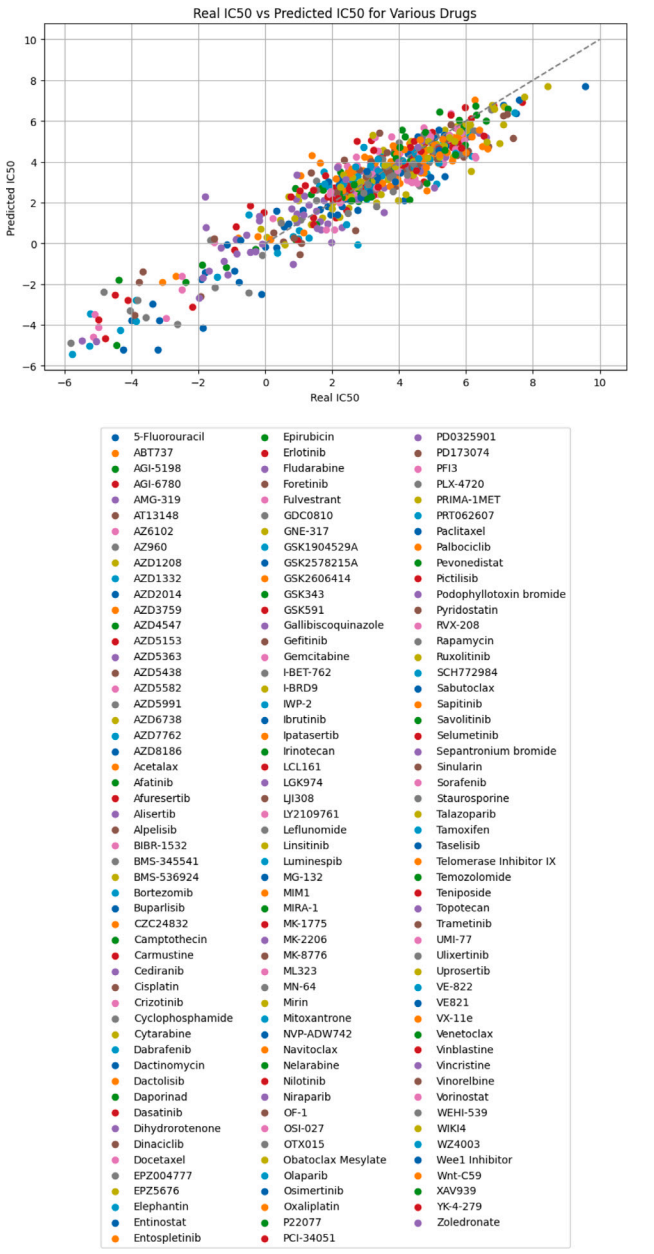


Fig. 13. Linear regression analysis of real versus predicted IC50 values of various drugs on GBM cancer.

with real values of IC50 in GBM samples. The mode of real values is from 4.5502 to 9.5503, whereas the predicted values are fall in 5.2502 to 7.7103. This proposes that though the model predict the tendency in IC50 values, there is spots of advancement (see Fig. 16).

Another drug named ABT737, the model succeeds for predicting the resistance, mostly real IC50 values around 2.213–4.324, but the proposed model obtained prediction difference such as 2.3820, where the predicted value was 3.3101. This shows the model's trend are acceptable for resistance prediction (see Fig. 17).

The chemo-drug AGI-6780, the model estimation were reasonably precise to the real IC50 values, demonstrate that the proposed model perform well for predicting the drug's resistance. The real IC50 values are in the bracket of 3.502 to 6.142, and the estimated values are very close to the real values of IC50 (see Fig. 18).

Some Drugs like AZD1332 and AZD8186 showed notable differences among real and predicted values. For the drug AZD1332, the trends of

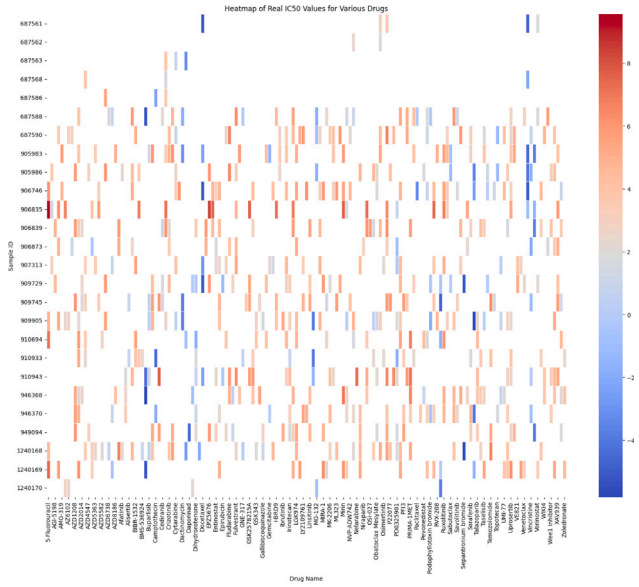


Fig. 14. Real IC50 values of different drugs.

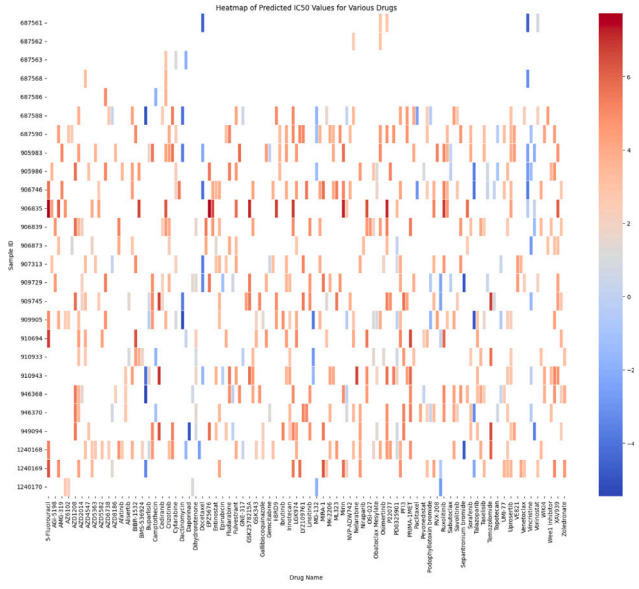


Fig. 15. Predicted IC50 values of different drugs.

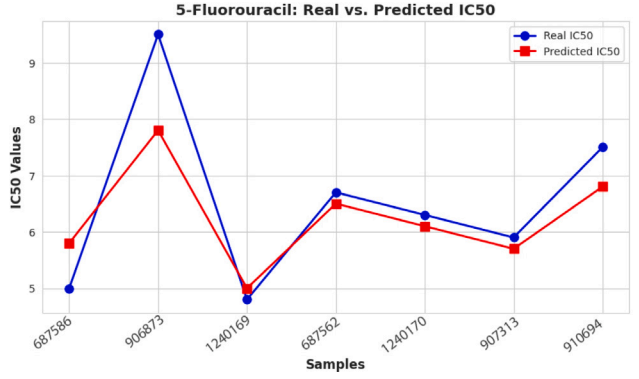


Fig. 16. Real and Predicted IC50 values of drug named 5-Fluorouracil.

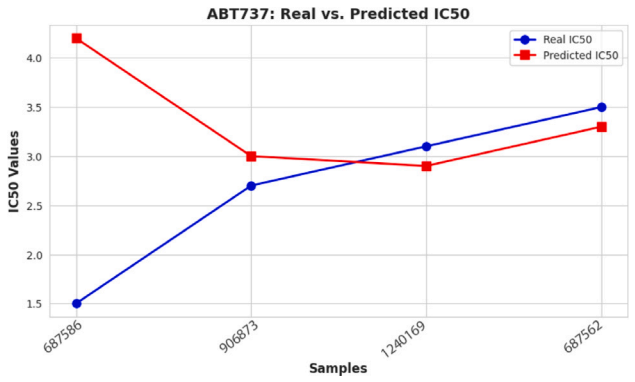


Fig. 17. Real and Predicted IC50 values of drug named ABT737.

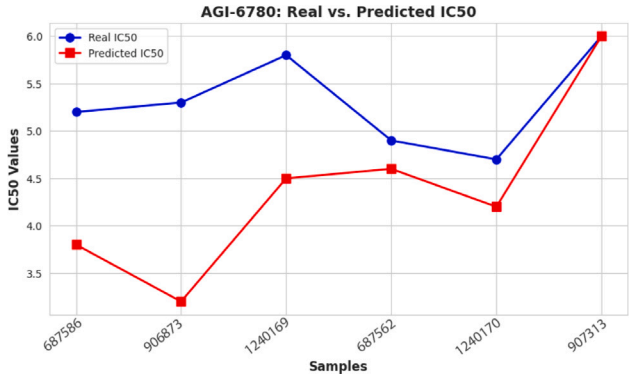


Fig. 18. Real and Predicted IC50 values of drug named AGI-6780.

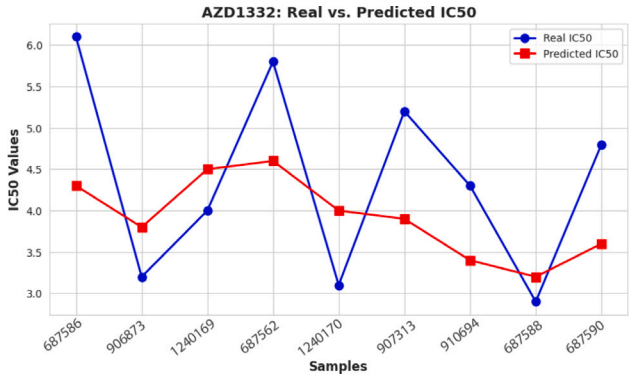


Fig. 19. Real and Predicted IC50 values of drug named AGI-6780.

IC50 values are different from real values, as real IC50 values are 6.160 and 1.751 and forecasted values are 4.272 and 3.513 respectively. Likewise, for AZD8186, the model usually miscalculated the IC50 values (see Figs. 19–20).

On the contrary, chemo-drugs such as Bortezomib and Dactinomycin, the proposed model achieved to retain a reliable estimation of drug resistance effectively. Such as, Bortezomib's real IC50 values vary between −5.771 to −4.342, and the estimated values sustained this tendency with values from −5.452 to −4.241, presenting the model's validity in managing negative IC50 values (see Figs. 21–22).

In the case of Cisplatin exhibited mixed effects, where the proposed model predicted the negative IC50 values accurately as well as positive values (see Fig. 23).

The proposed approach is competitive, often outperforming existing state-of-the-art models (see Table 1) regarding MSE, MAE, R^2, and

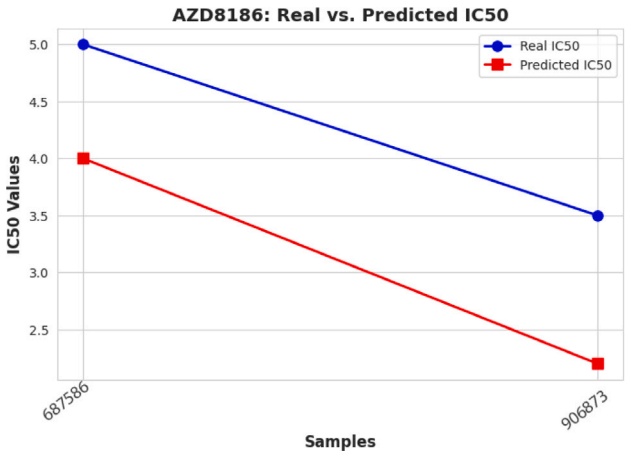


Fig. 20. Real and Predicted IC50 values of drug named AGI-6780.

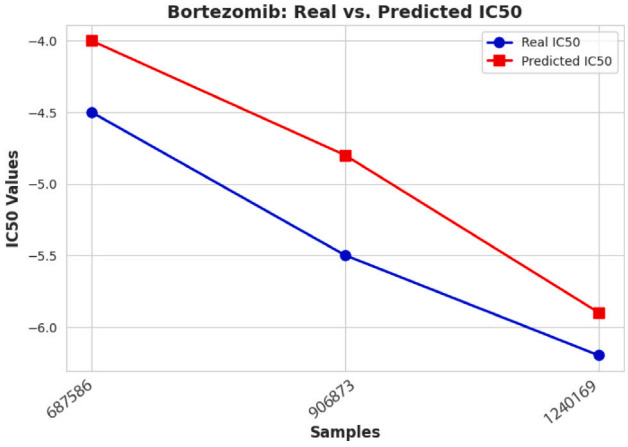


Fig. 21. Real and Predicted IC50 values of drug named Bortezomib.

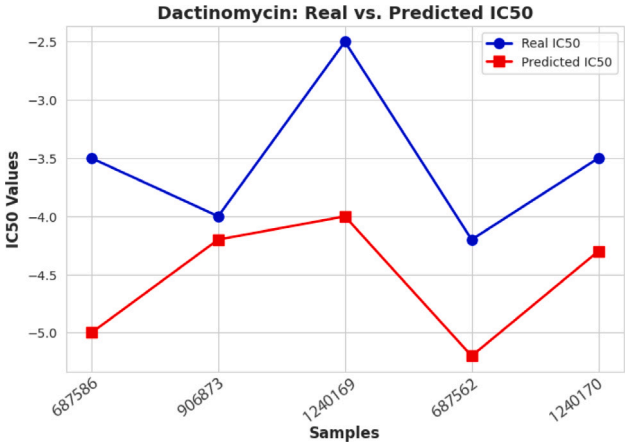


Fig. 22. Real and Predicted IC50 values of drug named Dactinomycin.

Pearson Correlation, demonstrating its significant ability to predict drug resistance with smaller error margins.

The proposed hybrid model works well because of the efficient preprocessing procedures we followed, such as normalizing the gene expression data and converting the SMILES strings to morgan fingerprints.

Our proposed model efficiently captures and combines comprehensive biological inputs using CNNs, LSTMs, and transforms. By employing tactics like lowering the plateau learning rate and stopping on the maximum learning point, we managed to prevent overfitting and ensured that our classifier was still reliable.

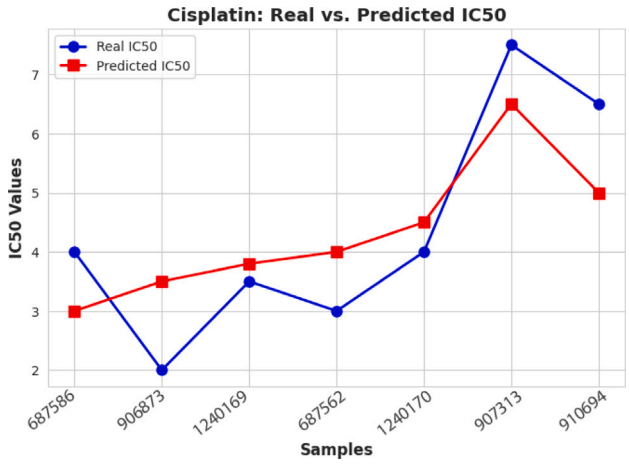


Fig. 23. Real and Predicted IC50 values of drug named Cisplatin.

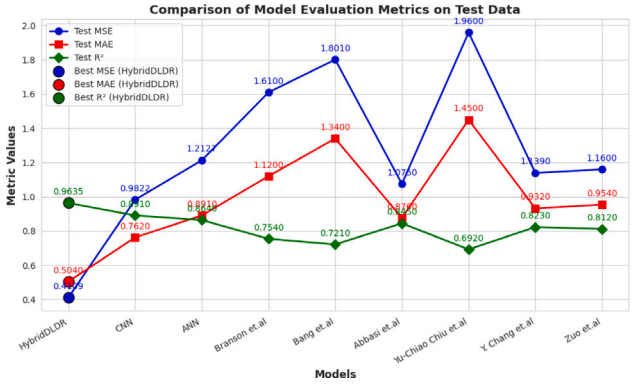


Fig. 24. Proposed model evaluation metrics on test data.

5. Discussion

The results show that the HybridDLDR model efficiently estimates drug resistance in GBM samples, emphasizing its novel fusion of CNN, LSTM, and Transformer architectures. This combination enables the proposed model to process multidimensional gene expression data and molecular descriptors, thereby influencing the model's ability for better forecasting accuracy. The model successfully estimating the inhibitory concentration for chemo-drugs such as 5-fluorouracil, ABT737, and AGI-6780, demonstrates its accuracy in analyzing drug-specific resistance. However, differences between actual and predicted IC50 values are detected in drugs such as AZD1332 and AZD8186. These miscalculations could be due to distinct data characteristics or drug properties that the model could not fully capture. The low MSE and MAE values, together with the high correlation values, highlight the strength of the model. Its ability to handle negative IC50 values for drugs such as bortezomib and dactinomycin further underlines its adaptability. The model's performance with cisplatin requires further exploration of how it manage drugs with varying IC50 distributions. One of the important aspects that contributed to the success of the model is the preprocessing approach, particularly the normalization of gene expression data and the transformation of SMILES strings into Morgan fingerprints. These preprocessing steps allowed the model to successfully manage multidimensional genetic data. In addition, training techniques such as reducing the learning rate on plateaus

and using early stopping helped to avoid overfitting and confirm reliable estimates across multiple datasets. Our model establishes strong analytical performance, it has some limitations that warrant further exploration. Foremost, discrepancies in estimation for specific drugs suggest that certain gene expression or molecular structures designs may not be well caught by the proposed model. Additionally, the model does not specifically handle noise or null values in the input data, which could affect robustness. Moreover, the computational complexity of training a hybrid CNN-LSTM-Transformer model poses challenges for huge amount of date processing. To address these problems in future work, we plan to incorporate more refined imputation techniques for managing null or missing data, explore domain adaptation strategies to decrease biases from heterogeneous data sources, and utilize model compression techniques such as pruning and quantization to enhance computational effectiveness. Generally, the HybridDLDR model provides a reasonable method for guessing chemo-resistance in GBM. Future work could concentrate on improving the estimation accuracy for chem-drugs such as AZD1332 and AZD8186 by integrating more nuanced data preprocessing.

5.1. Performance comparison with existing models

We compared our results with existing models to provide context. For example, (Branson et al. 2024) used a neural network-based model in their recent study. The researchers used a combination of gene expression data with molecular descriptors from GDSC dataset. The results showed an MSE of 1.61 [43] which is higher than proposed model.

Another model (Bang et al. 2024) merges molecular descriptors and gene expression using transfer learning. The results from this model show a cell line-blind test MSE value 1.801, and Pearson correlation value 0.883. The proposed model more efficient in MSE and pearson correlation as compare to Bang et al. [44].

To predict drug activity, another model (Abbasi et al. 2024) also integrates multiple data sources, including chemical structures and genomic data by using GDSC and PubChem. They achieved MSE value 1.075, which is higher than to proposed model and R^2 value 0.809 which is lower than proposed model [45].

In addition, a model (Yu-Chiao Chiu et al. 2019) incorporating several deep neural networks prediction methods there results shown as RMSE of 1.400 and MSE of 1.960 [46]. The researchers (Y. Chang et al. 2018) utilize deep neural networks and their results demonstrate as R^2 of 0.720, RMSE of 1.067, and MSE of 1.139 [47]. The researchers of (Zuo et al. 2021) achieved R^2 of 0.728, RMSE of 1.077, and MSE of 1.160 [48].

We confirmed the effectiveness of proposed model by accurately calculating drug resistance and comparing it with other existing models. Proposed model achieved lower MAE and MSE values, along with higher R^2, and Pearson correlation values (see Table 1) (see Figs. 25–26). This enhanced predictive power of the model arises from a hybrid method in which we integrate CNNs for molecular descriptors, while using LSTM applied to gene expression with transformer to understand complex interactions. (see Fig. 4).

We handle the training phase of the model using early stopping techniques and the Adam optimizer. These methods ensure the reliability and generalizability of proposed model.

5.2. Ablation study

To evaluate the individual contributions of deep learning components in our model, we conducted an ablation study by isolating and testing CNN, LSTM, and Transformer models. As shown in Table 2, the CNN achieved an MSE of 0.5123 and an R^2 of 0.9421. While CNNs are effective at capturing localized spatial features, they inherently lack mechanisms to account for long-range or sequential dependencies within gene expression profiles. This architectural limitation likely contributes to the CNN's comparatively higher MSE, as biological datasets often exhibit complex temporal and contextual interactions that require broader receptive fields.

The LSTM model improved upon this result, yielding an MSE of 0.4786 and an R^2 of 0.9507, due to its capacity to capture sequential dependencies through recurrent connections. The Transformer model further enhanced performance with an MSE of 0.4352 and an R^2 of 0.9592, leveraging its self-attention mechanism to model global relationships across gene features more effectively.

We further evaluated combinations of these architectures to investigate synergistic effects. The LSTM + Transformer model achieved an MSE of 0.4195, closely approaching the performance of our proposed HybridDLDR model. This is attributable to the complementary nature of LSTM and Transformer components, where LSTMs model sequential dynamics and Transformers contribute a broader contextual understanding. However, the HybridDLDR architecture goes a step further by incorporating CNN modules to capture localized patterns in addition to temporal and global features. This integrated tri-modular design results in the lowest MSE of 0.4109 and the highest R^2 of 0.9635, highlighting the benefit of unifying spatial, sequential, and contextual representations for robust prediction.

These findings underscore the significance of architectural diversity in modeling the multifaceted nature of drug response data and explain both the relatively weaker performance of CNN alone and the strong results obtained from LSTM+Transformer integration.

Table 1
Comparison of performances with existing models.

Models	MSE	R^2	Pearson correlation
HybridDLDR	0.4109	0.9635	0.9999
Naveed et al.-CNN [49]	0.9822	–	0.9151
Naveed et al.-ANN [49]	1.2127	–	0.9140
Branson et al. [43]	1.61	–	–
Bang el al. [44]	1.801	–	0.883
Abbasi et al. [45]	1.075	0.809	–
Yu-Chiao Chiu et al. [46]	1.960	–	–
Y. Chang et al. [47]	1.139	0.720	–
Zuo et al. [48]	1.160	0.728	–

Table 2
Ablation study: Performance comparison of individual and combined deep learning components. HybridDLDR achieves the best results by integrating CNN, LSTM, and Transformer models.

Models	MSE	R^2	Pearson correlation
HybridDLDR	0.4109	0.9635	0.9999
CNN	0.5123	0.9421	0.9978
LSTM	0.4786	0.9507	0.9984
Transformer	0.4352	0.9592	0.9991
CNN + LSTM	0.4507	0.9553	0.9987
CNN + Transformer	0.4289	0.9608	0.9990
LSTM + Transformer	0.4195	0.9621	0.9992

5.3. Evaluating the effect of artificial gene ordering

To address concerns regarding the use of CNN and LSTM models on gene expression data, specifically the lack of inherent biological ordering in gene features, we conducted a perturbation study to evaluate the impact of gene order on model performance. While gene expression profiles do not possess a natural sequence, models like CNNs and LSTMs require structured inputs. Therefore, we initially applied a consistent ordering based on gene IDs for reproducibility. However, to ensure that our results are not biased by any artificial ordering, we performed a robustness analysis through random gene order permutation.

We randomly permuted the order of gene expression features across all samples for 50 independent runs. For each permutation, the model

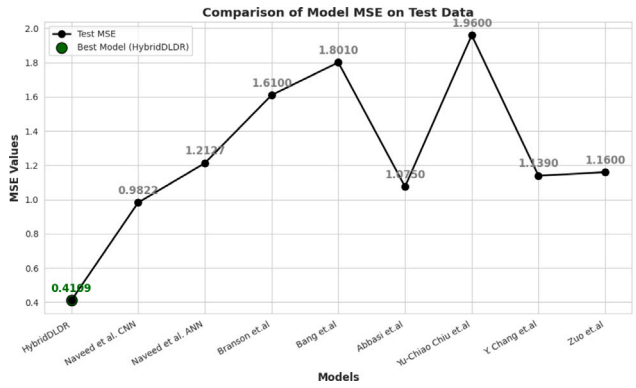


Fig. 25. Comparison of MSE on Test Data with existing models.

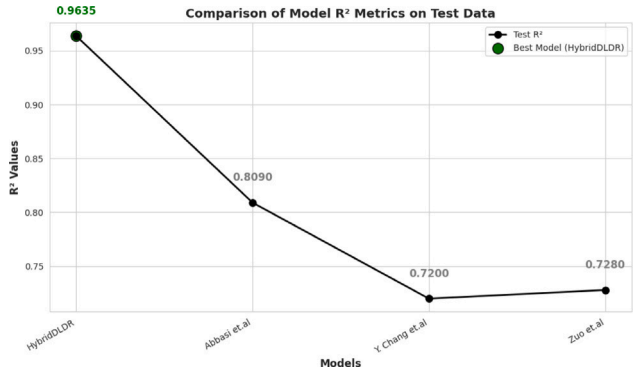


Fig. 26. Comparison of R^2 on Test Data with existing models.

Table 3
Impact of gene order perturbation on model performance.

Metric	Original order	Random order	Std. Dev.
MSE	0.4109	0.4152	±0.0063
Pearson Corr.	0.9999	0.9998	±0.0001
R^2	0.9635	0.9612	±0.0024

was retrained from scratch using the same architecture, hyperparameters, and data splits as in the main experiments. We evaluated the performance using MSE, PCC, and R^2 on the test set for each run (Table 3).

Across the 50 permutations, the model maintained stable performance. The standard deviation in MSE was found to be low (e.g., ±0.0063), and no notable differences were observed between the performance metrics of the original gene order and randomly ordered genes. This demonstrates that the model does not rely on any specific gene ordering for its predictive

5.4. Potential real-world applications

The proposed deep learning model holds significant promise for real-world applications, particularly in clinical decision-support systems (CDSS) and drug development pipelines.

5.4.1. CDSS

- The model can support medical practitioners and oncologists by predicting drug effectiveness based on gene expression.
- Precision medicine recommendations can be produced by assessing the molecular characteristics of a cancer and proposing the most effective drug.
- Incorporation with electronic health record (EHR) systems can allow real-time decision-making, refining treatment accuracy for cancer.

5.4.2. Drug development and precision medicine

- Pharmacological firms can take advantage of the model for *in silico* screening of drug candidates, accelerating the prediction of the most effective drug without lab tests.
- The capability to calculate IC_{50} values based on genomic data and chemical structures allows for effective ordering of drug candidates, enhancing lead compound selection.

6. Conclusion and future work

A noteworthy development has been made in drug resistance prediction with proposed hybrid deep learning-based resistance prediction system. By integrating gene expression data and molecular descriptors with CNNs, LSTMs, and transformers, we created a powerful tool that could enhance personalized medicine strategies. The proposed hybrid model demonstrates an acceptable estimation of drug resistance, learn tendency in IC50 values for several chemo-drugs. Although, the results accuracy varied drug to drug differently due to lack of data and noise in samples. The results showed a capable way for fit in composite deep learning models for resistance prediction, and play a role in precision medicine for efficacious malignance medical treatment.

We are committed to further improving our model, exploring various data types, and testing its performance with different datasets in the future.

7. Limitations

Certain limitations of the model, containing discrepancies in predictions for particular drugs such as AZD1332 and AZD8186, as well as possible issues rising from noise in the drug response and gene expression data. While regularization and dropout techniques aid mitigate overfitting, the model's generalizability to unseen drug composites remains undefined. Furthermore, inconsistency in genes, such as batch effects in gene expression profiling or dissimilarities in experimental conditions, may effect model performance.

CRediT authorship contribution statement

Sajid Naveed: Validation, Software, Methodology, Data curation. **Mujtaba Husnain:** Visualization, Supervision. **Najah Alsubaie:** Funding acquisition, Formal analysis.

Ethics statement

This study adheres to the highest ethical standards in research and data handling. The data used in this research were obtained from publicly available sources, ensuring compliance with ethical guidelines and regulatory requirements. No human or animal subjects were involved, and no personally identifiable information was utilized. All methodologies were implemented with transparency, reproducibility, and integrity to contribute meaningfully to scientific advancements in drug resistance prediction for glioblastoma.

Declaration of competing interest

I am writing to formally declare that I have no known competing financial interests or personal relationships that could have appeared to influence the work reported in the manuscript.

Acknowledgments

This research was funded by Princess Nourah bint Abdulrahman University Researchers Supporting Project number (PNURSP2025R321), Princess Nourah bint Abdulrahman University, Riyadh, Saudi Arabia).

Data availability

The source code and dataset for this study are publicly available to ensure reproducibility and further research. Researchers can access the implementation and related resources via the following GitHub repository:

GitHub Repository: https://github.com/xajidnaveedofficial/HybridDLDR.git.

The dataset is also accessible at: https://www.cancerrxgene.org/.

References

[1] Michael M. Gottesman, Robert W. Robey, Suresh V. Ambudkar, New mechanisms of multidrug resistance: An introduction to the cancer drug resistance special collection, Cancer Drug Resist. 6 (3) (2023) 590.

[2] Jiao Meng, Wei Qian, Zhenkun Yang, Lingli Gong, Daxing Xu, Hongbo Huang, Xinyi Jiang, Zhening Pu, Ying Yin, Jian Zou, P53/E2f7 axis promotes temozolomide chemoresistance in glioblastoma multiforme, BMC Cancer 24 (1) (2024) 317.

[3] Silvia Mara Baez Rodriguez, Amira Kamel, Gheorghe Vasile Ciubotaru, Gelu Onose, Ani-Simona Sevastre, Veronica Sfredel, Suzana Danoiu, Anica Dricu, Ligia Gabriela Tataranu, An overview of EGFR mechanisms and their implications in targeted therapies for glioblastoma, Int. J. Mol. Sci. 24 (13) (2023) 11110.

[4] Emir Begagić, Ragib Pugonja, Hakija Bečulić, Amila Čeliković, Lejla Tandir Lihić, Samra Kadić Vukas, Lejla Čejvan, Rasim Skomorac, Edin Selimović, Belma Jaganjac, et al., Molecular targeted therapies in glioblastoma multiforme: a systematic overview of global trends and findings, Brain Sci. 13 (11) (2023) 1602.

[5] Agata Gozdz, Proteasome inhibitors against glioblastoma—Overview of molecular mechanisms of cytotoxicity, progress in clinical trials, and perspective for use in personalized medicine, Curr. Oncol. 30 (11) (2023) 9676–9688.

[6] Maria F. Gonzalez-Aponte, Anna R. Damato, Laura Lucía Trebucq, Tatiana Simon, Sandra P. Cárdenas-García, Kevin Cho, Gary J. Patti, Diego A. Golombek, Juan José Chiesa, Joshua B Rubin, et al., Circadian regulation of MGMT expression and promoter methylation underlies daily rhythms in TMZ sensitivity in glioblastoma, J. Neurooncol. 166 (3) (2024) 419–430.

[7] Hongli Gao, Zhuo Xi, Jingwei Dai, Jinqi Xue, Xin Guan, Liang Zhao, Zhiguang Chen, Fei Xing, Drug resistance mechanisms and treatment strategies mediated by ubiquitin-specific proteases (USPs) in cancers: new directions and therapeutic options, Mol. Cancer 23 (1) (2024) 88.

[8] Antonio Passaro, Maise Al Bakir, Emily G. Hamilton, Maximilian Diehn, Fabrice André, Sinchita Roy-Chowdhuri, Giannis Mountzios, Ignacio I. Wistuba, Charles Swanton, Solange Peters, Cancer biomarkers: Emerging trends and clinical implications for personalized treatment, Cell 187 (7) (2024) 1617–1635.

[9] Malia Alexandra Foo, Mingliang You, Shing Leng Chan, Gautam Sethi, Glenn K. Bonney, Wei-Peng Yong, Edward Kai-Hua Chow, Eliza Li Shan Fong, Lingzhi Wang, Boon-Cher Goh, Clinical translation of patient-derived tumour organoids-bottlenecks and strategies, Biomark. Res. 10 (1) (2022) 10.

[10] Dipak D. Gadade, Hariom Jha, Chetan Kumar, Farzan Khan, Unlocking the power of precision medicine: exploring the role of biomarkers in cancer management, Futur. J. Pharm. Sci. 10 (1) (2024) 5.

[11] Harini Karimanal, Dinesh Bandaru, A review on integration of precision medicine in oncology practice, J. Pharma Insights Res. 2 (3) (2024) 016–022.

[12] Albrecht Stenzinger, Ejner K. Moltzen, Eva Winkler, Fruzsina Molnar-Gabor, Nisar Malek, Alexandru Costescu, Brigitte Nybo Jensen, Frédérique Nowak, Carmine Pinto, Ole Petter Ottersen, et al., Implementation of precision medicine in healthcare—A European perspective, J. Intern. Med. 294 (4) (2023) 437–454.

[13] Åsa Johansson, Ole A. Andreassen, Søren Brunak, Paul W. Franks, Harald Hedman, Ruth J.F. Loos, Benjamin Meder, Erik Melén, Craig E. Wheelock, Bo Jacobsson, Precision medicine in complex diseases—Molecular subgrouping for improved prediction and treatment stratification, J. Intern. Med. 294 (4) (2023) 378–396.

[14] Pratik Lamichhane, Anushka Agrawal, Precision medicine and implications in medical education, Ann. Med. Surg. 85 (4) (2023) 1342–1345.

[15] Xinyu Cao, Xu Zhou, Fei Hou, Yu-e Huang, Mengqin Yuan, Min Long, Sina Chen, Wanyue Lei, Jicun Zhu, Jiahao Chen, et al., ncRNADrug: a database for validated and predicted ncRNAs associated with drug resistance and targeted by drugs, Nucleic Acids Res. 52 (D1) (2024) D1393–D1399.

[16] Weixiong Pang, Ming Chen, Yufang Qin, Prediction of anticancer drug sensitivity using an interpretable model guided by deep learning, BMC Bioinformatics 25 (1) (2024) 182.

[17] Muhammad Dawood, Quoc Dang Vu, Lawrence S. Young, Kim Branson, Louise Jones, Nasir Rajpoot, Fayyaz ul Amir Afsar Minhas, Cancer drug sensitivity prediction from routine histology images, NPJ Precis. Oncol. 8 (1) (2024) 5.

[18] Qingqing Zhou, Yamei Wang, Chenqi Xin, XiaoMing Wei, Yuan Yao, Liang Xia, Identification of telomere-associated gene signatures to predict prognosis and drug sensitivity in glioma, Comput. Biol. Med. 168 (2024) 107750.

[19] Cui-Xiang Lin, Yuanfang Guan, Hong-Dong Li, Artificial intelligence approaches for molecular representation in drug response prediction, Curr. Opin. Struct. Biol. 84 (2024) 102747.

[20] Benjamin Haibe-Kains, Wail Ba-alawi, Abstract LB519: Bimodality of gene expression in cancer patients as interpretable biomarkers for drug sensitivity, Cancer Res. 82 (12_Supplement) (2022) LB519–LB519.

[21] Hossein Sharifi-Noghabi, Soheil Jahangiri-Tazehkand, Petr Smirnov, Casey Hon, Anthony Mammoliti, Sisira Kadambat Nair, Arvind Singh Mer, Martin Ester, Benjamin Haibe-Kains, Drug sensitivity prediction from cell line-based pharmacogenomics data: guidelines for developing machine learning models, Brief. Bioinform. 22 (6) (2021) bbab294.

[22] Heewon Park, Rui Yamaguchi, Seiya Imoto, Satoru Miyano, Xprediction: Explainable EGFR-TKIs response prediction based on drug sensitivity specific gene networks, Plos One 17 (5) (2022) e0261630.

[23] Danielle Maeser, Robert F. Gruener, Robert Galvin, Adam Lee, Tomoyuki Koga, Florina-Nicoleta Grigore, Yuta Suzuki, Frank B. Furnari, Clark Chen, R. Stephanie Huang, Integration of computational pipeline to streamline efficacious drug nomination and biomarker discovery in glioblastoma, Cancers 16 (9) (2024) 1723.

[24] Xuan Lin, Lichang Dai, Yafang Zhou, Zu-Guo Yu, Wen Zhang, Jian-Yu Shi, Dong-Sheng Cao, Li Zeng, Haowen Chen, Bosheng Song, et al., Comprehensive evaluation of deep and graph learning on drug–drug interactions prediction, Brief. Bioinform. 24 (4) (2023) bbad235.

[25] Xiao-Ying Liu, Xin-Yue Mei, Prediction of drug sensitivity based on multi-omics data using deep learning and similarity network fusion approaches, Front. Bioeng. Biotechnol. 11 (2023) 1156372.

[26] Bicna Song, Lumen Chao, Xiaolong Cheng, Yuan Gao, Ruocheng Shan, Wei Li, Abstract LB069: Predictive modeling of drug sensitivity based on the genetic dependency, Cancer Res. 83 (8_Supplement) (2023) LB069–LB069.

[27] Minwoo Pak, Sangseon Lee, Inyoung Sung, Bonil Koo, Sun Kim, Improved drug response prediction by drug target data integration via network-based profiling, Brief. Bioinform. 24 (2) (2023) bbad034.

[28] Xiaoyi Dong, Jianmin Bao, Ting Zhang, Dongdong Chen, Weiming Zhang, Lu Yuan, Dong Chen, Fang Wen, Nenghai Yu, Baining Guo, Peco: Perceptual codebook for bert pre-training of vision transformers, in: Proceedings of the AAAI Conference on Artificial Intelligence, vol. 37, (no. 1) 2023, pp. 552–560.

[29] Ziqiao Meng, Peilin Zhao, Yang Yu, Irwin King, Doubly stochastic graph-based non-autoregressive reaction prediction, 2023.

[30] Hao Xu, Zhengyang Zhou, Pengyu Hong, Graph multi-similarity learning for molecular property prediction, 2024, arXiv preprint arXiv:2401.17615.

[31] Hadrien Calmet, Damien Dosimont, David Oks, Guillaume Houzeaux, Brenda Vara Almirall, Kiao Inthavong, Machine learning and sensitivity analysis for predicting nasal drug delivery for targeted deposition, Int. J. Pharm. 642 (2023) 123098.

[32] Shaoyan Shi, Qian Wang, Xiaolong Du, Comprehensive bioinformatics analysis reveals the oncogenic role of FoxM1 and its impact on prognosis, immune microenvironment, and drug sensitivity in osteosarcoma, J. Appl. Genet. 64 (4) (2023) 779–796.

[33] Xiangqian Zhang, Yun Li, Yongheng Chen, Development of a comprehensive gene signature linking hypoxia, glycolysis, lactylation, and metabolomic insights in gastric cancer through the integration of bulk and single-cell RNA-seq data, Biomedicines 11 (11) (2023) 2948.

[34] Qi Wang, Chuanhua Zheng, Hanjin Hou, Xin Bao, Huading Tai, Xufeng Huang, Zhengrui Li, Zhangzuo Li, Qiaowei Wang, Qi Pan, et al., Interplay of sphingolipid metabolism in predicting prognosis of gbm patients: Towards precision immunotherapy, J. Cancer 15 (1) (2024) 275.

[35] Hao Chen, Yuanyong Wang, Changjian Shao, Kai Guo, Guanglin Liu, Zhaoyang Wang, Hongtao Duan, Minghong Pan, Peng Ding, Yimeng Zhang, et al., Molecular subgroup establishment and signature creation of lncrnas associated with acetylation in lung adenocarcinoma, Aging (Albany NY) 16 (2) (2024) 1276.

[36] Yiwen Lu, Ruixue Chen, Han Zhang, Xu Sun, Xiangjun Li, Mengyuan Yang, Xudong Zhang, Prognostic significance and immunological role of HPRT1 in human cancers, Biomol. Biomed. 24 (2) (2024) 262.

[37] Yiyun Pan, FangFang Xie, Wen Zeng, Hailong Chen, Zhengcong Chen, Dechang Xu, Yijian Chen, T cell-mediated tumor killing sensitivity gene signature-based prognostic score for acute myeloid leukemia, Discov. Oncol. 15 (1) (2024) 121.

[38] Shiqi Wang, Jiahui Wu, Qingcheng Wang, Yunfeng Zhang, Hong Yuan, Jianding Wang, Yonghui Wu, Yaxi Xu, Na Ji, Bin Quan, et al., Evaluation of a miniature mass spectrometer based point-of-care-test method for direct analysis of amlodipine and benazepril in whole blood, J. Pharm. Biomed. Anal. 245 (2024) 116194.

[39] Sajid Naveed, Mujtaba Husnain, A drug recommendation system based on response prediction: Integrating gene expression and K-mer fragmentation of drug SMILES using LightGBM, Intell. Based Med. (ISSN: 2666-5212) 11 (2025) 100206.

[40] Jian Zhou, Housheng Zheng, Huiru Zhang, Wenqiang Yu, Baoer Li, Liang Ye, Lu Wang, MCM5 is a novel therapeutic target for glioblastoma, OncoTargets Ther. (2024) 371–381.

[41] Wanjuan Yang, Jorge Soares, Patricia Greninger, Elena J. Edelman, Howard Lightfoot, Simon Forbes, Nidhi Bindal, Dave Beare, James A. Smith, I. Richard Thompson, et al., Genomics of drug sensitivity in cancer (GDSC): a resource for therapeutic biomarker discovery in cancer cells, Nucleic Acids Res. 41 (D1) (2012) D955–D961.

[42] National Cancer Institute, (NCI) and the National Human Genome Research Institute, (NHGRI), The cancer genome atlas program TCGA, 2016, https://www.cancer.gov/ccg/research/genome-sequencing/tcga.

[43] Nikhil Branson, Pedro R. Cutillas, Conrad Bessant, Comparison of multiple modalities for drug response prediction with learning curves using neural networks and XGBoost, Bioinform. Adv. 4 (1) (2024) vbad190.

[44] Dongmin Bang, Bonil Koo, Sun Kim, Transfer learning of condition-specific perturbation in gene interactions improves drug response prediction, Bioinformatics 40 (Supplement_1) (2024) i130–i139.

[45] Maryam Abbasi, Filipa G. Carvalho, Bernardete Ribeiro, Joel P. Arrais, Predicting drug activity against cancer through genomic profiles and SMILES, Artif. Intell. Med. 150 (2024) 102820.

[46] Yu-Chiao Chiu, Hung-I Harry Chen, Tinghe Zhang, Songyao Zhang, Aparna Gorthi, Li-Ju Wang, Yufei Huang, Yidong Chen, Predicting drug response of tumors from integrated genomic profiles by deep neural networks, BMC Med. Genom. 12 (2019) 143–155.

[47] Yoosup Chang, Hyejin Park, Hyun-Jin Yang, Seungju Lee, Kwee-Yum Lee, Tae Soon Kim, Jongsun Jung, Jae-Min Shin, Cancer drug response profile scan (CDRscan): a deep learning model that predicts drug effectiveness from cancer genomic signature, Sci. Rep. 8 (1) (2018) 8857.

[48] Zhaorui Zuo, Penglei Wang, Xiaowei Chen, Li Tian, Hui Ge, Dahong Qian, SWnet: a deep learning model for drug response prediction from cancer genomic signatures and compound chemical structures, BMC Bioinformatics 22 (2021) 1–16.

[49] Sajid Naveed, Mujtaba Husnain, Ali Samad, Amna Ikram, Hina Afreen, Ghulam Gilanie, Najah Alsubaie, Drug efficacy recommendation system of glioblastoma (GBM) using deep learning, IEEE Access 13 (2025) 10398–10411.